Applications of μc-SiO_x:H as integrated n-layer and back transparent conductive oxide for a-Si:H/μc-Si:H tandem cells

2014 Jpn. J. Appl. Phys. 53 05FV08

(http://iopscience.iop.org/1347-4065/53/5S1/05FV08)

Japanese Journal of Applied Physics **53**, 05FV08 (2014) **REGULAR PAPER**
http://dx.doi.org/10.7567/JJAP.53.05FV08

Applications of μc-SiO_x:H as integrated n-layer and back transparent conductive oxide for a-Si:H/μc-Si:H tandem cells

Shin-Wei Liang*, Yen-Tang Huang, Hung-Jung Hsu, Cheng-Hang Hsu, and Chuang-Chuang Tsai

Department of Photonics and Institute of Electro-Optical Engineering, National Chiao Tung University, Hsinchu 300, Taiwan, R.O.C.
E-mail: singwayshepherd@gmail.com

Received November 27, 2013; accepted February 27, 2014; published online April 22, 2014

We have prepared n-type hydrogenated microcrystalline silicon oxide [μc-SiO_x:H(n)] films with oxygen contents from 0 to 37.3 at. % by varying the CO_2-to-SiH_4 flow ratio in a plasma-enhanced chemical vapor deposition (PECVD) system. By using μc-SiO_x:H(n) as an effective replacement for integrated μc-Si:H(n) and indium–tin oxide (ITO), μc-Si:H single-junction and a-Si:H/μc-Si:H tandem cells exhibited significantly improved efficiencies of 6.35 and 10.53%, respectively. The improvement of the single-junction and tandem cells mainly arose from the enhancement of long-wavelength optical absorption in μc-Si:H absorbers, which was confirmed by a quantum efficiency instrument showing a markedly enhanced spectral response at wavelengths from 600 to 1100 nm. Moreover, all the PECVD processes, except the metal contact, had an advantage of in situ deposition without breaking vacuum, thereby minimizing contamination of the interface. The simplified cell fabrication can enhance the fill factor, which will benefit industrial production.

1. Introduction

Hydrogenated microcrystalline silicon (μc-Si:H) has been developed and introduced as an intrinsic photovoltaic absorbing material for silicon thin-film solar cell application.[1–7] Its enhanced absorption in the long-wavelength region and low-light-induced degradation compared with those of hydrogenated amorphous silicon (a-Si:H) are the major advantages of integrating μc-Si:H into solar cells. The common stacked cell configuration is the a-Si:H/μc-Si:H tandem-junction cell, which consists of wider-bandgap amorphous silicon (a-Si:H) as the top absorber and narrower-bandgap μc-Si:H as the bottom absorber.[8–11] The a-Si:H absorber has to be kept reasonably thin to minimize the impact of light-induced degradation.[12,13] This makes well-controlled light management essential for maintaining or improving performance. Good light management can be achieved by increasing the light path in the absorber, allowing the use of thin active layers. To achieve adequate top-cell current, the optical absorption in the top cell can be increased using an intermediate reflecting layer between the top and bottom cells.[14–18]

Similarly, a relatively thick μc-Si:H absorber is generally required to achieve adequate absorption, with consequences of a decreased fill factor (FF) and an open-circuit voltage (V_{OC}) due to a weak internal electric field and an inefficient carrier transport.[7] To obtain sufficient bottom-cell current when using thinner absorbers, an effective approach is to enhance optical absorption using a back reflector to reflect unabsorbed photons back to the absorber. This highly reflective back reflector often consists of a transparent conductive oxide (TCO) and a metal contact.[19–21] The insertion of TCO is proposed to improve the refractive-index matching to silicon thin films and to reduce the parasitic absorption loss by the suppressed excitation of texture-mediated surface plasmonic resonance at the metal contact.[22] Nevertheless, the need for an ex situ TCO sputtering step was inevitable in the past. As an alternative, studies[23,24] have shown that n-type hydrogenated silicon oxide can replace back TCO as a back reflector to enhance the optical path in Si thin-film silicon solar cells. In addition to the replacement of back TCO, the use of n-type hydrogenated microcrystalline silicon oxide [μc-SiO_x:H(n)] as both n-type and back TCO layers in a-Si:H solar cells has been reported.[25,26] However, the optical reflection at long wavelengths (>700 nm) by the back reflector[23] cannot be efficiently utilized in a-Si:H cells owing to the low absorption at long wavelengths. Considering its dual function as the doped layer and back reflector, in this work, we employed a μc-SiO_x:H(n) film as a replacement for both n-type and back TCO layers in μc-Si:H single-junction and a-Si:H/μc-Si:H tandem cells.

The μc-SiO_x:H(n) material is a phase mixture of μc-Si:H and amorphous silicon oxide (a-SiO_x:H), where phosphorus doping mainly affects the μc-Si:H phase.[27–31] The n-type μc-Si:H phase ensures sufficient electrical conductivity in the direction of the current flow in the cell device, and the a-SiO_x:H phase with different oxygen contents supplies the lower refractive index and optical transparency.[27] Accordingly, the electrical and optical properties of μc-SiO_x:H films significantly depend on the oxygen content and crystallization. The bandgap (E_{04}) can be changed from slightly less than 2 to 2.9 eV, and the refractive index (n) determined from the wavelength of 1 μm can be controlled from approximately 3.8 (μc-Si:H) down to approximately 1.5, which is closed to the n of silicon dioxide.[27,30,31] Depending on the requirement of the devices, μc-SiO_x:H films can be prepared by considering the trade-off among crystallization, conductivity, n, and E_{04}.

2. Experimental procedure

Doped and undoped silicon-based thin films were prepared using a 27.12 MHz multi-chamber plasma-enhanced chemical vapor deposition (PECVD) system by a single-chamber process and NF_3 in situ plasma cleaning. n-Type μc-SiO_x:H thin films were deposited from a gas mixture of silane (SiH_4), hydrogen (H_2), phosphine (PH_3), and carbon dioxide (CO_2). Optical and electrical characterizations were performed on 150-nm-thick thin films deposited on glass. The oxygen content and crystalline volume fraction of μc-SiO_x:H films were examined by X-ray photoelectron spectroscopy (XPS) and Raman spectroscopy ($\lambda = 488$ nm), respectively. Electrical measurements were carried out to investigate the in-plane conductivity. The optical bandgap (E_{04}, the photon energy at which the absorption coefficient is $1 \times 10^4\,cm^{-1}$) of μc-SiO_x:H layers was obtained by ultraviolet–visible–infrared optical measurement. 1.2-μm-thick μc-Si:H single-

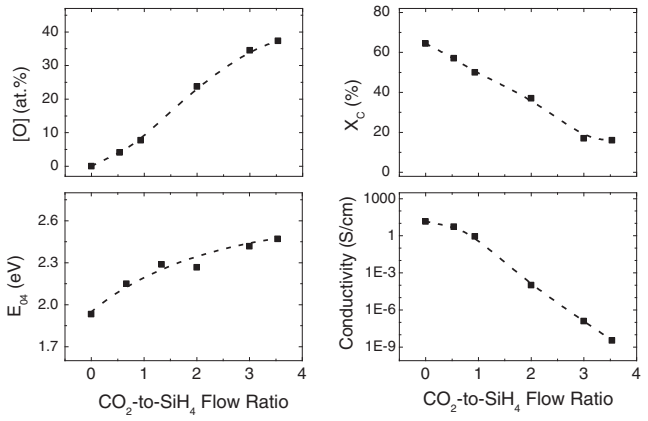

Fig. 1. Effects of CO_2-to-SiH_4 flow ratio (R_{CO2}) on oxygen content ([O]), bandgap (E_{04}), crystalline volume fraction (X_C), and conductivity (σ).

junction and a-Si:H/μc-Si:H tandem solar cells with a thickness of 0.24/1.4 μm were fabricated on commercial textured SnO_2:F glass with a superstrate configuration. The standard cells used for comparison consisted of sputtered indium–tin oxide (ITO), which was subsequently deposited on μc-Si:H(n) after being transferred in ambient. The solar cells with a patterned area of 0.25 cm^2 were characterized using an AM1.5G illuminated current density–voltage (J–V) measurement system and a quantum efficiency instrument.

3. Results and discussion

μc-SiO_x:H films with different oxygen contents have been deposited by varying the CO_2-to-SiH_4 flow ratio (R_{CO2}) in the range from 0 to 3.5. Figure 1 shows the effects of R_{CO2} on the oxygen content ([O]), bandgap (E_{04}), crystalline volume fraction (X_C), and conductivity (σ) of μc-SiO_x:H(n) films. The hydrogen dilution ratio (R_{H2}, defined as the ratio of hydrogen flow rate to the sum of silane and hydrogen flow rates) was maintained at 98.5% with a fixed PH_3 flow rate. As R_{CO2} increased from 0 to 3.5, [O] increased from 0 to 37.3 at. %. The introduced CO_2 is suggested to react with hydrogen to form an OH radical, which bonds to the film surface, thus, O is incorporated into the films.[32] With an increase in the amount of O incorporated, the increasing [O] decreased the refractive index ($\lambda = 632$ nm) from 3.8 to 2.3 (not shown) and increased E_{04} from 1.93 to 2.47 eV. In contrast, X_C and the conductivity both decreased as R_{CO2} increased. X_C decreased from 64 to 15%, and the corresponding conductivity decreased from 14 to 3×10^{-9} S/cm. The decrease in X_C was attributed to the increase in [O], which quenched the crystallization in the μc-SiO_x:H(n) films. By combining the effects of X_C and [O], the smaller amount of crystalline phase and the higher [O] led to a decrease in conductivity.

The characteristics of μc-SiO_x:H(n) films can be varied by adjusting different deposition parameters to achieve a wider bandgap and a lower refractive index, with acceptable conductivity compared with that of μc-Si:H(n). For the following solar cell applications, we employed a μc-SiO_x:H(n) film deposited under the following conditions: $R_{CO2} = 0.55$, $R_{H2} = 98.5\%$, and $PH_3/SiH_4 = 0.45\%$. The film properties are listed in Table I. To investigate the effect of μc-SiO_x:H(n) in solar cells, we first employed μc-SiO_x:H(n) to replace μc-Si:H(n) and ITO in a μc-Si:H single-junction solar cell. The cell structure is shown in Fig. 2.

Table I. μc-SiO_x:H(n) film properties for the following solar cell applications.

[O] (at. %)	σ (S/cm)	X_C (%)	E_{04} (eV)	n ($\lambda = 632$ nm)
4.4	5.31	57	2.0	3.6

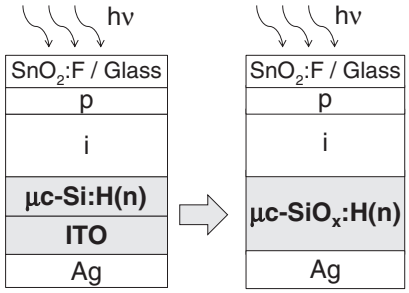

Fig. 2. Schematic diagram of the cell structure showing the replacement of μc-Si:H(n) and ITO by μc-SiO_x:H(n) in μc-Si:H single-junction solar cells.

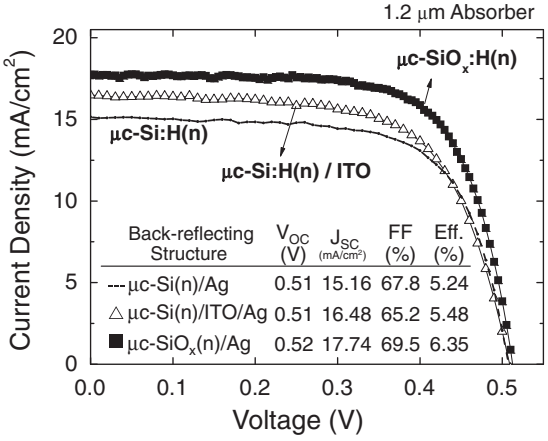

Fig. 3. J–V characteristics of μc-Si:H single-junction cells with different back-reflecting structures.

Figure 3 shows the J–V characteristics of μc-Si:H single-junction cells with different back-reflecting structures. The thickness of a μc-Si:H absorber was kept at 1.2 μm. Compared with the cell using μc-Si:H(n)/Ag back-reflecting structure, the cell using the μc-Si:H(n)/ITO/Ag structure had an apparent enhancement of short-circuit current density (J_{SC}) from 15.16 to 16.48 mA/cm^2 with only a slightly decreased fill factor (FF). The enhanced J_{SC} can be attributed to the refractive-index difference between silicon films and Ag that induced the optical reflection back into the absorber. One possible reason for the slightly decreased FF might be the ion bombardment damage during ITO sputtering and the degraded μc-Si:H(n)/ITO interface due to vacuum breaking and sputtering damage. Söderström et al. have also made a similar discussion regarding the interface damage issue.[33]

Compared with the cell using μc-Si:H(n)/ITO/Ag, the cell using μc-SiO_x:H(n)/Ag for replacing both μc-Si:H(n) and ITO showed an increase in FF and V_{OC}, with further increase in J_{SC} from 16.48 to 17.74 mA/cm^2. The significantly

Table II. Performance parameters of a-Si:H/μc-Si:H tandem-junction solar cells with different back-reflecting structures.

Bottom-cell n-layer	Back TCO	V_{OC} (V)	J_{SC} (mA/cm^2)	FF (%)	Eff. (%)	Top J_{SC} (mA/cm^2)	Bot. J_{SC} (mA/cm^2)	Total J_{SC} (mA/cm^2)
μc-Si:H(n)	None	1.35	9.33	72.6	9.15	11.22	9.50	20.72
μc-Si:H(n)	ITO	1.35	10.06	74.2	10.08	11.37	10.47	21.84
μc-SiO$_x$:H(n)		1.36	10.08	76.9	10.59	11.42	11.13	22.55

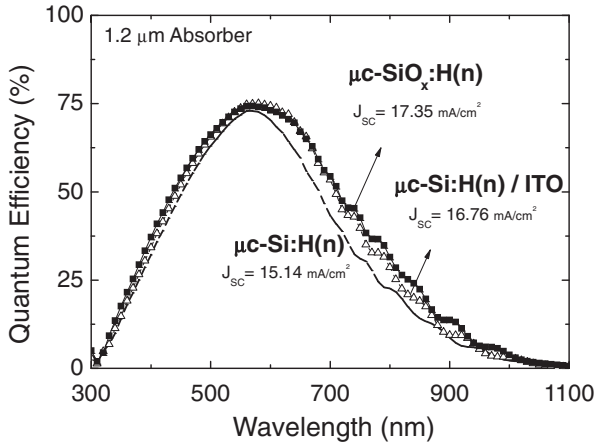

Fig. 4. Quantum efficiencies of μc-Si:H single-junction cells with different back-reflecting structures.

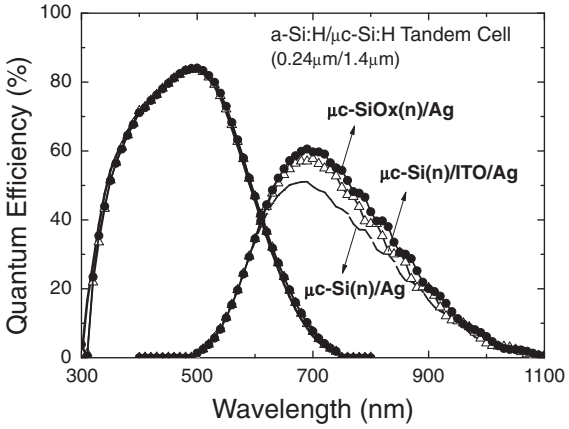

Fig. 5. Quantum efficiencies of a-Si:H/μc-Si:H tandem solar cells using different back-reflecting structures.

increased J_{SC} can be attributed to enhanced optical absorption in absorbers, as confirmed by a quantum efficiency instrument. This may arise from the additional optical reflection at the i/n interface due to the refractive-index difference between the μc-Si:H and μc-SiO$_x$:H(n) films. The increased V_{OC} may be due to the wider bandgap of μc-SiO$_x$:H(n) than of μc-Si:H(n), while the increased FF might be ascribed to in situ deposition in the PECVD chamber without breaking the vacuum, minimizing the contamination of the interface. The result showed that μc-SiO$_x$:H(n) can be an effective replacement for the integrated n-layer and ITO. It also has the advantage of process simplification and better interface quality without breaking vacuum. The conversion efficiency of the μc-Si:H single-junction cell using μc-SiO$_x$:H(n) as a replacement for μc-Si:H(n) and ITO improved to 6.35%, with $J_{SC} = 17.73\,\text{mA/cm}^2$, $V_{OC} = 0.52\,\text{V}$, and FF = 69.5%.

As shown in Fig. 4, the marked increase of J_{SC} in μc-Si:H single-junction cells was investigated by a quantum efficiency instrument. Compared with that of the cells using the μc-Si:H(n)/Ag and μc-Si:H(n)/ITO/Ag structures, that of the cells using the μc-SiO$_x$:H(n)/Ag structure showed a significant increase in the long-wavelength region of 600–1100 nm. This can be ascribed to the suppression of parasitic absorption loss in the n-type layer compared with the μc-Si:H(n) films and the refractive-index difference at the i/n interface to enhance the long-wavelength optical absorption in the absorber. As a result, the J_{SC} of quantum efficiency was enhanced to 17.35 mA/cm^2 using the μc-SiO$_x$:H(n)/Ag as a replacement for the μc-Si:H(n)/Ag or μc-Si:H(n)/ITO/Ag back-reflecting structures. All the PECVD processes, except the metal contact, can simplify the cell fabrication and result in comparable or even better device performance.

For a-Si:H/μc-Si:H tandem solar cells, we have also applied the μc-SiO$_x$:H(n)/Ag back-reflecting structure to achieve an improved light management. The a-Si:H/μc-Si:H tandem cell with a superstrate configuration consisted of a 0.24-μm-thick a-Si:H top cell and a 1.4-μm-thick μc-Si:H bottom cell. Table II shows the performance of an a-Si:H/μc-Si:H tandem solar cell using different back-reflecting structures. With the same a-Si:H top cell, the tandem cell using the μc-SiO$_x$:H(n)/Ag and μc-Si:H(n)/ITO/Ag structures exhibited observable improvements in J_{SC}, FF, and conversion efficiency as compared with the cell using the μc-Si:H(n)/Ag structure. Compared with the cell having the μc-Si:H(n)/ITO/Ag structure, the cell with the μc-SiO$_x$:H(n)/Ag structure showed slightly improved V_{OC} and FF, accompanied by a notable improvement in J_{SC}, which was confirmed by the quantum efficiency result shown in Fig. 5. No differences in the quantum efficiency were observed at short wavelengths, whereas a strong enhancement was obtained at wavelengths higher than 630 nm. In the μc-SiO$_x$:H(n)/Ag back-reflecting structure, the bottom-cell J_{SC} obtained from the quantum efficiency instrument increased from 10.47 to 11.13 mA/cm^2, as compared with that observed in the cell using the μc-Si:H(n)/ITO/Ag structure. The significant enhancement of the spectral response at wavelengths from 630 to 1100 nm was likely due to more enhanced long-wavelength optical reflection. The total current, defined as the sum of the top-cell current and bottom-cell current, increased from 20.72 to 22.55 mA/cm^2. The results indicate that μc-SiO$_x$:H(n) can be an effective replacement for both n-type and back TCO layers in the a-Si:H/μc-Si:H tandem cell. The conversion efficiency of the a-Si:H/μc-Si:H tandem cell using the μc-SiO$_x$:H(n)/Ag back-reflecting structure was improved to 10.59%, with $J_{SC} = 10.08\,\text{mA/cm}^2$, $V_{OC} = 1.36\,\text{V}$, and FF = 76.9%.

4. Conclusions

Phosphorus-doped hydrogenated microcrystalline silicon oxide [μc-SiO_x:H(n)] films with different oxygen contents have been prepared by varying the CO_2-to-SiH_4 flow ratio in a PECVD system. The oxygen content can be adjusted from 0 to 37.3 at. %, but is accompanied by a decreased conductivity from 14 to 3×10^{-9} S/cm. By using μc-SiO_x:H(n) as an effective replacement for integrated μc-Si:H(n) and ITO, the conversion efficiency of the μc-Si:H single-junction cell was improved to 6.35%, with $J_{SC} = 17.73\,mA/cm^2$, $V_{OC} = 0.52$ V, and FF = 69.5%. The a-Si:H/μc-Si:H tandem cell using a μc-SiO_x:H(n)/Ag back-reflecting structure exhibited a 10.59% initial efficiency, with $J_{SC} = 10.08\,mA/cm^2$, $V_{OC} = 1.36$ V, and FF = 76.9%. The major improvement of the single-junction and tandem cells arose from the enhancement of the long-wavelength optical absorption in μc-Si:H absorbers, which was confirmed by the quantum efficiency instrument showing a significantly increased spectral response at wavelengths from 600 to 1100 nm. By using the μc-SiO_x:H(n)/Ag back-reflecting structure, the enhanced fill factor in μc-Si:H single-junction and a-Si:H/μc-Si:H tandem-junction solar cell also showed the advantage of in situ deposition without breaking the vacuum, minimizing the contamination of the interface. All the PECVD processes, except the metal contact, simplified the cell fabrication, which will benefit the industrial production.

Acknowledgements

This work was supported by the National Science Council of Taiwan under grant number 102-3113-P-008-001.

1) C. Wang and G. Lucovsky, Proc. 21st IEEE Photovoltaic Specialists Conf., 1990, Vol. 2, p. 1614.
2) J. Meier, R. Flückiger, H. Keppner, and A. Shah, Appl. Phys. Lett. **65**, 860 (1994).
3) J. Meier, P. Torres, R. Platz, S. Dubail, U. Kroll, J. A. Anna-Selvan, N. Pellaton-Vaucher, C. Hof, D. Fischer, H. Keppner, and A. Shah, MRS Proc. **420**, 3 (1996).
4) A. H. M. Smets, T. Matsui, and M. Kondo, J. Appl. Phys. **104**, 034508 (2008).
5) K. Yamamoto, IEEE Trans. Electron Devices **46**, 2041 (1999).
6) S. Hänni, G. Bugnon, G. Parascandolo, M. Boccard, J. Escarré, M. Despeisse, F. Meillaud, and C. Ballif, Prog. Photovoltaics **21**, 821 (2013).
7) H. Sai, T. Koida, T. Matsui, I. Yoshida, K. Saito, and M. Kondo, Appl. Phys. Express **6**, 104101 (2013).
8) H. Takatsuka, M. Noda, Y. Yonekura, Y. Takeuchi, and Y. Yamauchi, Sol. Energy **77**, 951 (2004).
9) K. Yamamoto, A. Nakajima, M. Yoshimi, T. Sawada, S. Fukuda, T. Zuezaki, M. Ichikawa, Y. Koi, M. Goto, T. Meguro, T. Matsuda, M. Kondo, T. Sasaki, and Y. Tawada, Sol. Energy **77**, 939 (2004).
10) A. Shah, J. Meier, A. Buechel, U. Kroll, J. Steinhauser, F. Meillaud, H. Schade, and D. Dominé, Thin Solid Films **502**, 292 (2006).
11) S. Guha and J. Yang, J. Non-Cryst. Solids **352**, 1917 (2006).
12) D. Staebler and C. Wronski, Appl. Phys. Lett. **31**, 292 (1977).
13) M. Stutzmann, W. B. Jackson, and C. C. Tsai, Phys. Rev. B **32**, 23 (1985).
14) D. Fischer, S. Dubail, J. A. A. Selvan, N. P. Vaucher, R. Platz, Ch. Hof, U. Kroll, J. Meier, P. Torres, H. Keppner, N. Wyrsch, M. Goetz, A. Shah, and K.-D. Ufert, Proc. 25th IEEE Photovoltaic Specialists Conf., 1996, p. 1053.
15) P. Buehlmann, J. Bailat, D. Dominé, A. Billet, F. Meillaud, A. Feltrin, and C. Ballif, Appl. Phys. Lett. **91**, 143505 (2007).
16) P. Obermeyer, C. Haase, and H. Stiebig, Appl. Phys. Lett. **92**, 181102 (2008).
17) V. Smirnov, A. Lambertz, B. Grootoonk, R. Carius, and F. Finger, J. Non-Cryst. Solids **358**, 1954 (2012).
18) S.-T. Hwang, D. J. You, S. H. Kim, S. Lee, and H.-M. Lee, Sol. Energy Mater. Sol. Cells **113**, 79 (2013).
19) K. Hayashi, K. Masataka, A. Ishikawa, and H. Yamaguchi, Proc. 1st IEEE World Conf. Photovoltaic Energy Conversion, 1994, p. 674.
20) E. Terzini, A. Rubino, R. de Rosa, and M. Addonzonio, MRS Proc. **377**, 681 (1995).
21) S. S. Hegedus, W. A. Buchanan, and E. Eser, Proc. 26th IEEE Photovoltaic Specialists Conf., 1997, p. 603.
22) F. J. Haug, T. Söderström, O. Cubero, V. Terrazzoni-Daudrix, and C. Ballif, J. Appl. Phys. **104**, 064509 (2008).
23) S. Y. Myong and L. S. Jeon, Sol. Energy Mater. Sol. Cells **119**, 77 (2013).
24) S. Kim, H. Lee, J.-W. Chung, S.-W. Ahn, and H.-M. Lee, Curr. Appl. Phys. **13**, 743 (2013).
25) P. D. Veneri, L. V. Mercaldo, and I. Usatii, Appl. Phys. Lett. **97**, 023512 (2010).
26) Y. P. Lin, Y. W. Tseng, S. W. Liang, C. H. Hsu, and C. C. Tsai, presented at 2012 MRS Spring Meet., 2012.
27) A. Lambertz, T. Grundler, and F. Finger, J. Appl. Phys. **109**, 113109 (2011).
28) D. Das, M. Jana, and A. K. Barua, Sol. Energy Mater. Sol. Cells **63**, 285 (2000).
29) A. Sarker, C. Banerjee, and A. K. Barua, J. Phys. D **35**, 1205 (2002).
30) T. Grundler, A. Lambertz, and F. Finger, Phys. Status Solidi C **7**, 1085 (2010).
31) V. Smirnov, O. Astakhov, R. Carius, Y. Petrusenko, V. Borysenko, and F. Finger, Jpn. J. Appl. Phys. **51**, 022301 (2012).
32) D. Das, S. M. Iftiquar, and A. K. Barua, J. Non-Cryst. Solids **210**, 148 (1997).
33) T. Söderström, F.-J. Haug, X. Niquille, and C. Ballif, Prog. Photovoltaics **17**, 165 (2009).